Hindawi
International Journal of Photoenergy
Volume 2022, Article ID 8632826, 13 pages
https://doi.org/10.1155/2022/8632826

Research Article

Numerical Study on the Optimization Design of Photovoltaic/Thermal (PV/T) Collector with Internal Corrugated Channels

Xiangrui Kong[1], **Yuhan Zhang**[2], **Jinshun Wu**[1] and **Song Pan**[3]

[1]*School of Architecture Engineering, North China Institute of Science and Technology, Yanjiao, 065201, China*
[2]*Beijing Uni-Construction Group Company, LTD, Beijing 100029, China*
[3]*School of Civil Engineering and Architecture, Beijing University of Technology, Beijing 100022, China*

Correspondence should be addressed to Jinshun Wu; wujinshun2005@163.com

Received 19 March 2022; Revised 1 August 2022; Accepted 5 September 2022; Published 17 September 2022

Academic Editor: Congcong Wang

Copyright © 2022 Xiangrui Kong et al. This is an open access article distributed under the Creative Commons Attribution License, which permits unrestricted use, distribution, and reproduction in any medium, provided the original work is properly cited.

This study presents a theoretical study on the super thin and conductive thermal absorber with built-in corrugated channels on the basis of previous field experiments. The flow and heat transfer characteristics of the corrugated channels are simulated to identify the factors affecting photovoltaic/thermal (PV/T) system efficiency. The influences of the structural parameters such as the corrugation number, the corrugation area, and the flow channel width on the water outlet temperature and heat collection are discussed in order to support the structural optimization design of the hybrid PV/T system. The simulation results were validated to be in good agreement with experimental results. The results indicate that increasing inlet water velocity leads to a decrease in the outlet temperature. It was found that the corrugation area and the flow channel width have impacts on the outlet temperature of the hybrid PV/T collector panel. When the flow channel width of the absorber plate is reduced from 4 mm to 3 mm, the outlet temperature attained is between 298 and 302 K, and the heat collection is in the range of 16.2–51.4 MJ/h. This led to an increase in the amount of heat collected by 18.6%.

1. Introduction

The solar photovoltaic/thermal (PV/T) system is one of the key research focuses of the solar energy utilization field due to its high thermal energy output and comprehensive utilization compared with PV or solar thermal systems alone [1, 2]. It was widely used in several industries, like power generation stations [3–5], dryers [6, 7], building heating [8, 9, 10], and desalination systems [11–13]. In recent years, great progress has been made in the optimization and application of solar photovoltaic/thermal (PV/T) systems. No matter in what field the PV/T system is used, improving its performance is the key and final objective. Many studies have been conducted to investigate the PV/T system performance involving utilizing PCM [14–16], using nanofluids [17, 18], concentrated application [19, 20], and air and water configurations [1, 21, 22] by various methodologies such as experimental, analytical, numerical, and simulation techniques. Due to the structure and performance improvement of the heat collector having a great influence on the whole PV/T system components' efficiency, technologies for this purpose, including the cooling channel design or modifications of the PV/T systems, have been developed substantially. This includes using single and double pass and using fins, suspended plates, concentrating plates, etc.

Hissouf et al. [23] investigated the theoretical performance of a PV/T solar collector employing three different geometrical shapes of fluid circulation channels (circular tube, half tube, and square tube) and a heat transfer fluid of pure water and ethylene glycol-water (EG-W) mixture. The half tube design is found to provide the best photovoltaic cooling effect and the highest efficiency. The use of pure water as working fluid improves thermal and electrical yields by 4.5% and 1.85%, respectively, compared to the EG-W mixture. A new type (double pass) of photovoltaic/thermal panel and a novel latent heat storage unit integrated with the condenser of the heat pump were designed and manufactured in Kosan and Aktas' study [8]. The numerical analysis was performed using the Ansys Fluent program to characterize the thermal behavior of the phase change material in the latent heat storage unit.

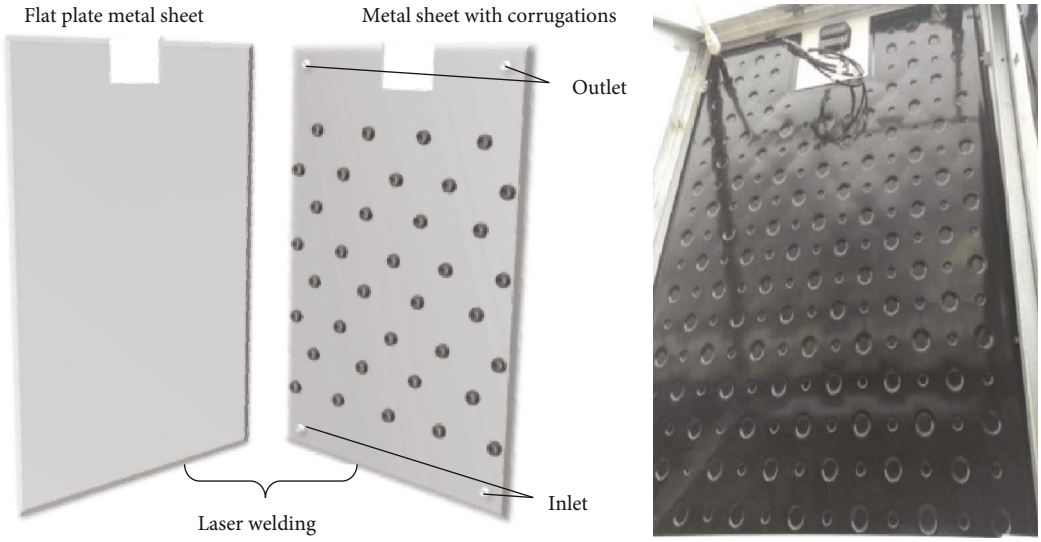

Figure 1: Schematic of the thermal absorber (a) and the associated PV/T prototypes (b).

Table 1: Relevant parameters of the heat absorber plate core.

Items	Parameters
Absorber plate material	Iron
Large corrugation's diameter	35 mm, 25 mm
Small corrugation's diameter	20 mm, 15 mm
Inlet/outlet diameters	20 mm
Inlet/outlet lengths	50 mm
Flow channel width	4 mm

Table 2: Material parameters.

Items	Density (kg/m^3)	Specific heat volume (J/kg·K)	Thermal conductivity (W/m·K)	Coefficient viscosity (kg/m)
Water	998.2	4182	0.6	0.001003
Iron	8030	502.48	16.27	—

It was observed that the heat pump system's average coefficient of performance varied between 2.93 and 3.18. The photovoltaic/thermal panel was able to store 1.07 kWh of electrical energy and produce 9.59% more electricity than the photovoltaic panel alone. Yu et al. [24] investigated a novel solar Micro-Channel Loop-Heat-Pipe Photovoltaic/Thermal (MC-LHP-PV/T) system through experimental measurements. A prototype MC-LHP-PV/T system employing R-134a as working fluid was designed and measured to evaluate its solar thermal and electrical efficiencies and its impact factors. The results found that a lower inlet water temperature, a higher water flow rate, a higher ambient temperature, and a larger height difference between the condenser and the evaporator can help to increase the solar thermal efficiency of the system. Compared to existing PV/T and BIPV/T systems, the new MC-LHP-PV/T system achieved 17.20% and 33.31% higher overall solar efficiency. By utilizing numerical and experimental approaches, Çiftçi et al. [25] developed and analyzed a vertical hybrid PV/T solar dryer. Their results showed that the thermal efficiency values of the finned vertical PV/T collector were much higher than those of the finless vertical PV/T collector. The sustainability index values of finless and finned drying systems were between 2.16-2.75 and 2.38-3.25, respectively. Arslan et al. [26] designed a new type of finned air fluid photovoltaic/thermal collector and performed numerical and experimental analysis on it. It was reported that 0.42% improvement in electrical efficiency occurred due to the cooling of PV. The average thermal and electrical efficiency obtained for the PV/T was 49.5% and 13.98%, respectively, with a mass flow rate of 0.04553 kg/s. To achieve higher thermal and electrical efficiencies, Yao et al. [27] designed and optimized the fluid channel pattern of the solar-assisted PV/T heat pump. The optimized two-phase flow channel pattern had significant improvements in temperature uniformity, thermal and electrical efficiencies, and hydraulic behavior. Fan et al. [28] developed a multiobjective design optimization strategy for hybrid photovoltaic/thermal collector- (PV/T-) solar air heater (SAH) systems with fins to maximize thermal energy generation and net electricity gains. To improve the cooling capacity and required pump power of parallel cooling channels (PCCs), Yu et al. [29] studied the heat transfer in parallel cooling channels with periodically expanded grooves (PEGs).

The hybrid photovoltaic/thermal (PV/T) collector with internal corrugated channels studied in this work has the characteristics of using pass or fins mentioned above. It was developed by Xu et al. [30] to retrofit the existing PV panel into a photovoltaic/thermal (PV/T) panel. The current study is thus built up on top of the previously reported works in the literature [30, 31] which conducted a parallel comparative investigation on the PV and PV/T panel systems through both laboratory and field experiments. The previous study [30] has shown that the electrical efficiency of the PV/T unit can be improved by 16.8% through the

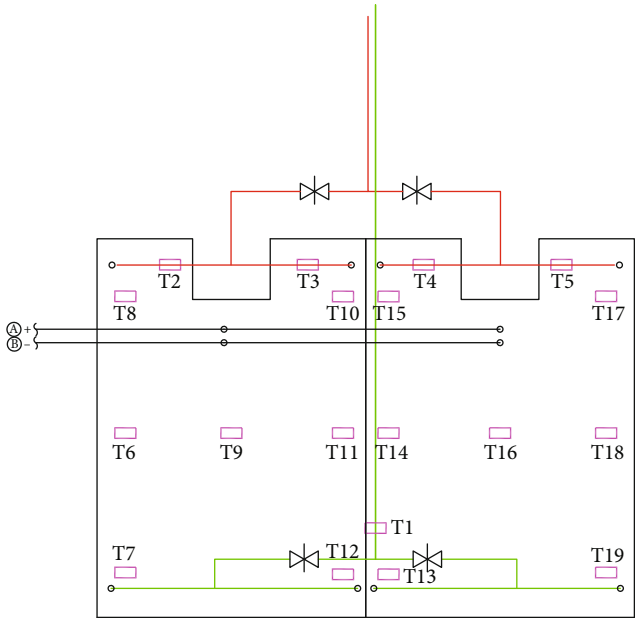

Figure 2: Location of the measuring points set on the absorber plate.

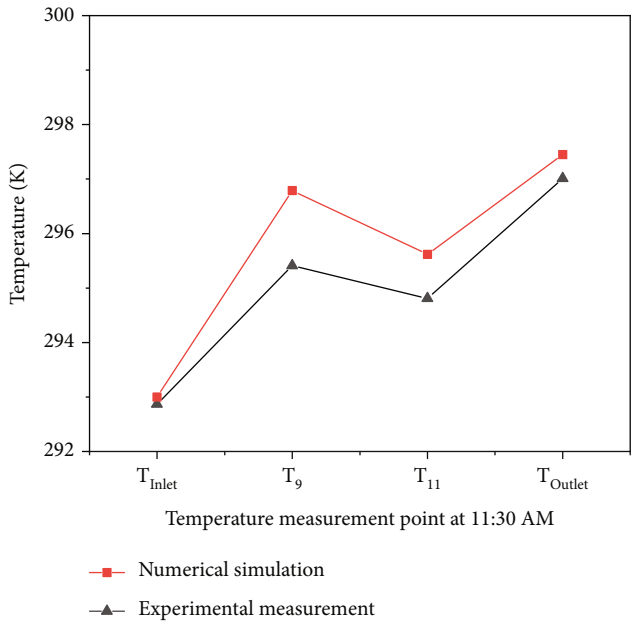

Figure 3: Temperature comparison of different measurement points between experimental measurements and numerical simulation.

use of a super thin-conductive thermal absorber, and the thermal efficiency reaches 65%. Compared with the same PV, the hybrid PV/T panel could enhance the electrical return by nearly 3.5% and increase the overall energy output by nearly 324.3%.

The overall energy output of hybrid PV/T panels is mainly related to heat collection efficiency. To improve the efficiency of solar energy conversion of PV/T systems, it is necessary to investigate the factors affecting the heat transfer performance of the absorber plate. The geometric characteristics of the absorber plate are also key factors affecting the internal flow and heat transfer characteristics. In addition, the optimized structural parameters should meet the demands of different sizes and thicknesses of a wall body and installation convenience. However, it is difficult to achieve the temperature and velocity of the working medium in the plate through laboratory measurements and identify the influence of factors on the absorber plate's heat transfer performance due to its complex structure. In this work, a CFD model of the super thin-conductive thermal absorber was established on the basis of the previous field experiment [31]. The flow and heat transfer characteristics of the corrugated channels are simulated to identify the key factors affecting the PV/T system efficiency. Finally, the influences of the structural parameters, such as corrugation areas, corrugation numbers, and flow channel width, on the flow and heat transfer characteristics are discussed to support the structural optimization design of the hybrid PV/T panel with corrugated cooling channels.

2. Methodology

2.1. Photovoltaic/Thermal (PV/T) Panel with Corrugated Cooling Channels. The PV/T in this article is designed by attaching the PV panel to a super thin-conductive thermal absorber through a series of U-shaped resilient metal clips. The thermal absorber was laser-welded together through two parallel thin flat plate metal sheets with a 1 mm thickness. One sheet was extruded by a machinery mold to formulate arrays of mini corrugations while the other sheet remained smooth. These two metal sheets form the built-in turbulent flow channels with a 4 mm width, which engenders high heat transfer capacity. The corner holes are cut on the four corners of the corrugated sheet as the working medium water's inlet and outlet channels with a spacing of 4 cm. The physical map and plane schematic diagram of the heat-absorbing core are shown in Figure 1, and the relevant parameters of the heat absorber plate are shown in Table 1.

2.2. Mathematical Model. In this article, a CFD model was established using the hybrid PV/T panel with large and small corrugations as the research objects. To simplify the simulation, the following assumptions are made:

(1) The irradiance, ambient temperature, and inlet water temperature are constant

(2) The working medium water is considered to be an incompressible liquid

(3) The materials' properties are constant

(4) The flow is fully developed

The solid boundary involved in the simulation model is iron. The physical property parameters of water and iron are shown in Table 2. The same boundary condition as in the reference experiment [31] was adopted; that is, the front of the collector was kept as a constant heat source.

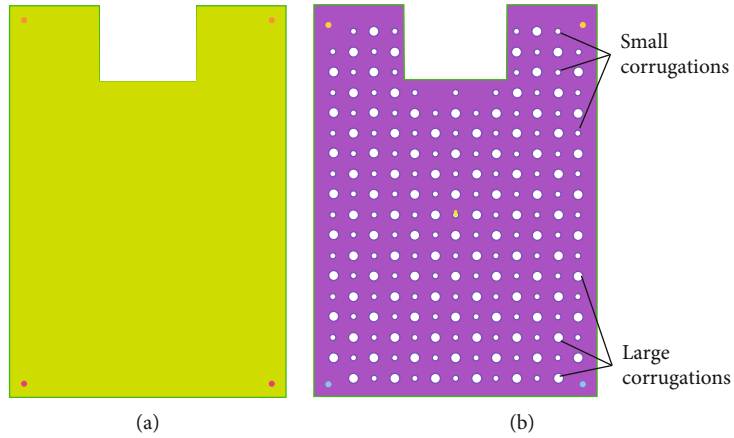

Figure 4: The metal sheet with smooth surface (a) and metal sheet with corrugations (b).

2.2.1. Model Equations. Considering that the heat absorber is an ultrathin type of superconducting tablet, the internal flow of fluid had streamline curvature and vortex due to the corrugations. The fluid was affected largely by the wall in the internal, and its turbulence developed insufficiently near the wall surface. The realizable k-ε model was chosen for this study because it more accurately predicts the performance of the flat plate absorber. Its specific expression was as follows:

$$\rho\frac{\partial k}{\partial \tau}+\rho u_j\frac{\partial k}{\partial x_i}=\frac{\partial}{\partial x_i}\left[\left(\mu+\frac{\mu_t}{\sigma_k}\right)\frac{\partial k}{\partial x_j}\right]+G_k+G_b-\rho\varepsilon-Y_M+S_k, \tag{1}$$

where ρ and μ are the density and viscosity of the water, respectively; τ is the time; k is the turbulent energy; μ_t is the turbulent viscosity; x_i and x_j are the displacement in the x and y directions, respectively; u and v are the velocity of water along the x and y axis, respectively; G_k is the turbulent kinetic energy term that is generated by the laminar velocity gradient; G_b is the turbulent kinetic energy term that is generated by buoyancy; ε is the turbulent dissipation rate; Y_M refers to the wave generated by the transition diffusion in compressible turbulence; S_k is defined as the turbulent kinetic energy; and σ_k is the turbulent Prandtl number in the k equation.

The governing equation for the dissipation ratio ε is as follows:

$$\rho\frac{\partial \varepsilon}{\partial \tau}+\rho u_j\frac{\partial \varepsilon}{\partial x_j}=\frac{\partial}{\partial x_j}\left[\left(\mu+\frac{\mu_t}{\sigma_\varepsilon}\right)\frac{\partial \varepsilon}{\partial x_j}\right]+\rho C_1 S_\varepsilon-\rho C_2\frac{\varepsilon^2}{k+\sqrt{\nu\varepsilon}}+C_{1\varepsilon}\frac{\varepsilon}{k}C_{3\varepsilon}G_k+S_\varepsilon \tag{2}$$

where σ_ε is the turbulent Prandtl number in ε equation, S_ε is defined as the turbulent dissipation source, $C_{1\varepsilon}$ and C_2 are constants, and $C_{3\varepsilon}$ is the influence term of buoyancy on the dissipation rate:

$$C_1=\max\left[0.43,\frac{\eta}{\eta+5}\right],\qquad \eta=S\frac{k}{\varepsilon}, \tag{3}$$

where S is the influence term of average strain rate on turbulence.

2.2.2. Numerical Method and Boundary Conditions. The ICEM module of commercial computational fluid dynamics (CFD) software Ansys Fluent was used to establish the geometric model and carry out the structural mesh division. Three-dimensional single precision was selected. The SIMPLE algorithm and an uncoupled implicit solver were used for the solution. The heat transfer surface grid encryption technology, boundary layer mesh technology, and general grid interface (GGI) mesh link technology were used. Grid independence verification was also conducted. When the number of grids is about 2.17 million, the outlet temperature error is less than 2%.

For the incompressible flow in channels, the following boundary conditions are set according to the actual operating conditions of the experimental platform [31]:

(1) The inlet velocity v ranges from 0.2 to 1.5 m/s, and the inlet water temperature T_{in} is 293 K

(2) The outlet was the outflow of quality

(3) The wall surface was chosen to be made of iron. To simplify the simulation, when simulating the influence of temperature difference on the water's flow and heat transfer characteristics inside the plate, all the wall surfaces were assumed adiabatic, except the outer heating surface, which was set at a corresponding constant temperature

2.3. Model Validation. To validate the numerical model developed in this work, the numerical simulation results

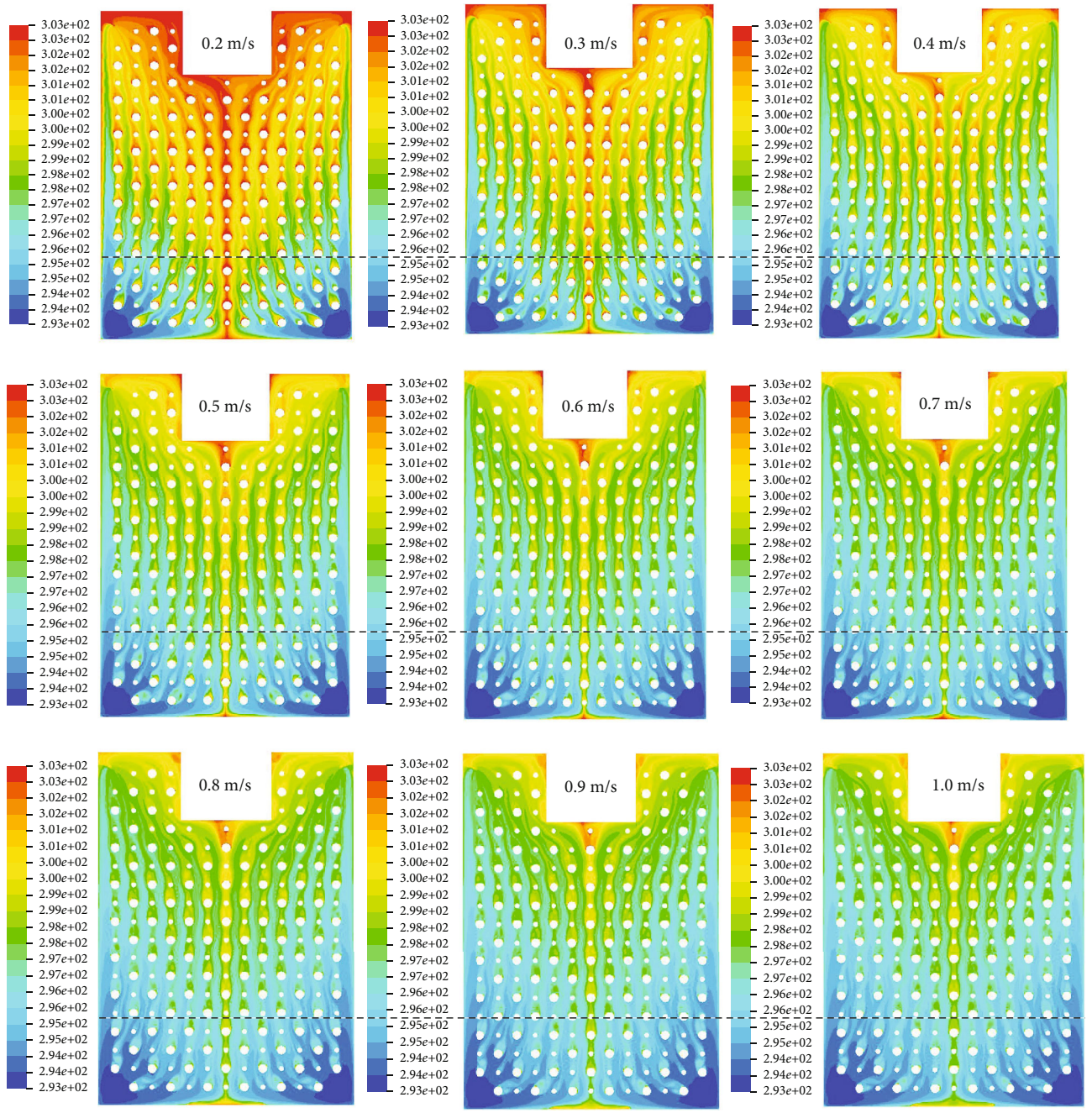

Figure 5: Temperature distribution (in K) at different inlet flow velocities.

for the inlet water temperature, the outlet temperature, and the temperature near the plate center (T9) and two sides (T11), considering an inlet flow velocity of 1.5 m/s, are compared with the experimental data from Li et al. [31]. The experimental temperature was obtained by setting 14 measuring points (T6-T19) on the back board of the hybrid plate (as shown in Figure 2). The minimum and maximum temperatures recorded by the temperature sensor are -323~473 K, respectively. At 11:30, it is noted that the experimental and numerical simulation inlet water temperatures are approximate and are selected for comparison, as illustrated in Figure 3.

Overall, the temperature distribution at the different measurement points is similar in the case of experimental and numerical simulations. The maximum reported discrepancy is around 0.5%, exhibited at point T9. The differences may be due to the positions of the experimental measurement points. The flow channel is too narrow to install a temperature monitor to get the temperature of the water inside. Except for the inlet and outlet temperatures, the rest of the measuring points are arranged on the back board of the hybrid plate during the experiment. The thermal absorber is made up of two super thin metal sheets. It was considered that the back board temperature is approximately equal to

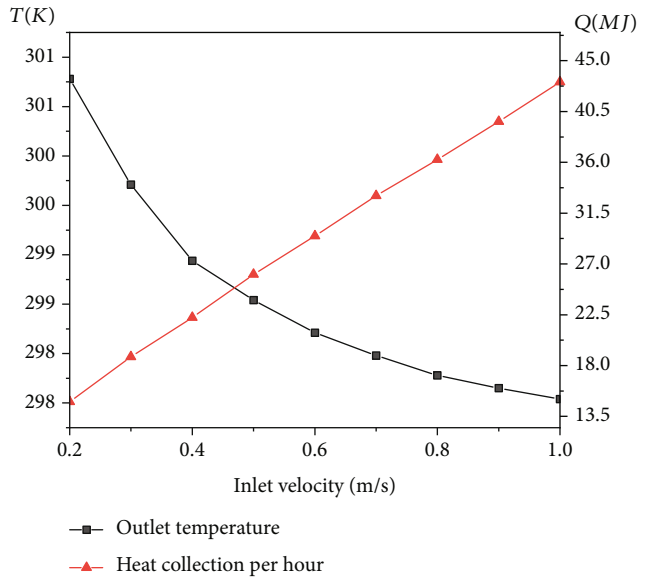

Figure 6: Outlet temperature and hourly heat collection of heat absorber.

the internal water temperature at steady state conditions. It is noted that when the inlet flow velocity is high, the rate of heat removal from the PV panel is low, which leads to insufficient heat transfer by the internal working medium. Therefore, the simulated outlet temperature is higher than the experimentally measured one. In a previous study presented in the literature [22], the water outlet temperature was found to drop as the inlet water velocity increased. In general, the temperature distributions by simulation show reasonable agreement with the test results. Hence, the numerical model can accurately predict the heat transfer of the hybrid absorber's internal flow channels.

3. Results and Discussions

This study firstly analyzed the flow and heat transfer characteristics of the water in the present absorber plate under different inlet velocities and heating surface temperatures. Then, the flow and heat transfer characteristics were simulated by changing the structural parameters of the hybrid PV/T panel, such as corrugation numbers, corrugation areas, and flow channel width, while other conditions were maintained constant. Finally, the optimization direction was given by comparing it with the previous hybrid heat collector and the flat plate heat collector. The flat plate collector is laser-welded together by two parallel metal sheets with a smooth surface (Figure 4(a)). The hybrid collector is laser-welded together by two parallel metal sheets. One sheet has corrugations (Figure 4(b)), while the other sheet remains smooth.

3.1. Effect of the Internal Temperature and Inlet Velocity. When the inlet velocity is greater than 1.0 m/s, the water outlet temperature drops very little. The water outlet temperature is 297.54 K when the inlet flow velocity is 1.0 m/s, and it drops to 297.45 K when the inlet flow velocity is 1.5 m/s. The temperature distribution in the parallel heating surface direction is similar. Therefore, in order to identify the influence of inlet velocity and heating surface temperature on the heat absorber, this study simulated the water temperature and velocity distributions at different conditions: the inlet velocity was increased by a 0.1 m/s increment from 0.2 to 1.0 m/s, and the heating surface temperature was 298, 303, 308, and 313 K, respectively. The geometry parameters and other conditions are constant.

The water temperature inside the PV/T panel drops as the inlet water velocity increases (Figure 5). At a low inlet flow velocity (0.2 m/s), it can be seen that the water temperature is high due to the fact that the rate of heat removal from the PV panel is high at low inlet flow rates. The temperature distribution in the parallel heating surface direction is similar no matter how the water inlet velocity changes (Figure 5). The temperature near the plate exit is high, while the part near the entrance is low. The temperature of the absorber plate is symmetrical about the symmetry axis, and the temperature on both sides is lower than at the center.

According to the temperature difference between the collector inlet and outlet, heat collection at different water inlet velocities can be obtained (Figure 6). The outlet temperature decreases with the increase in the water inlet velocities. This is due to the fact that at low flow velocities, the working fluid will take more time to absorb heat from a PV panel compared to the case at high speeds. In general, increasing the flow rate will lead to a decrease in the PV temperature [32], and thus, the rate of heat removal from the PV panel is thus low. As the inlet velocity increases, the heat collection per hour increases, and the amplitude decreases gradually. When the velocity varies from 0.2 to 1.0 m/s, the heat collection is in the range of 14.8-43.1 MJ/h.

Figure 7 shows the water temperature distribution at different heating surface temperatures with water inlet velocity being 0.5 m/s. All the temperature distributions at different heating surfaces have a similar trend. The temperature near the middle is slightly higher than it is on either side. The temperatures near the two exits are high, and the temperatures near the entrances are low. This may also be due to the flow velocity distribution of the working medium inside the plate (Figure 8). The water velocity on both sides is high, while it is low near the middle part. Compared to the sides, the water in the middle has a longer flow path and a lower velocity. This relatively low velocity, along with the high rate of heat removal from the PV panel, results in sufficient heat exchange between the PV panel and the water.

Figure 9 shows the outlet temperature and heat collection under different heating surface temperatures with the inlet velocity being 0.5 m/s. The outlet temperature and heat collection per hour increase with the rise of the heating surface temperatures. The trend is linear, and the rate is decreasing. Under this condition, the outlet temperature of the heat collector is between 298 and 313 K, and the heat collection per hour is in the range of 12.3~53.5 MJ. An increase in the PV panel temperature leads to an increase in the outlet temperature due to the rise in the work medium temperature, which was also reported in the study conducted by

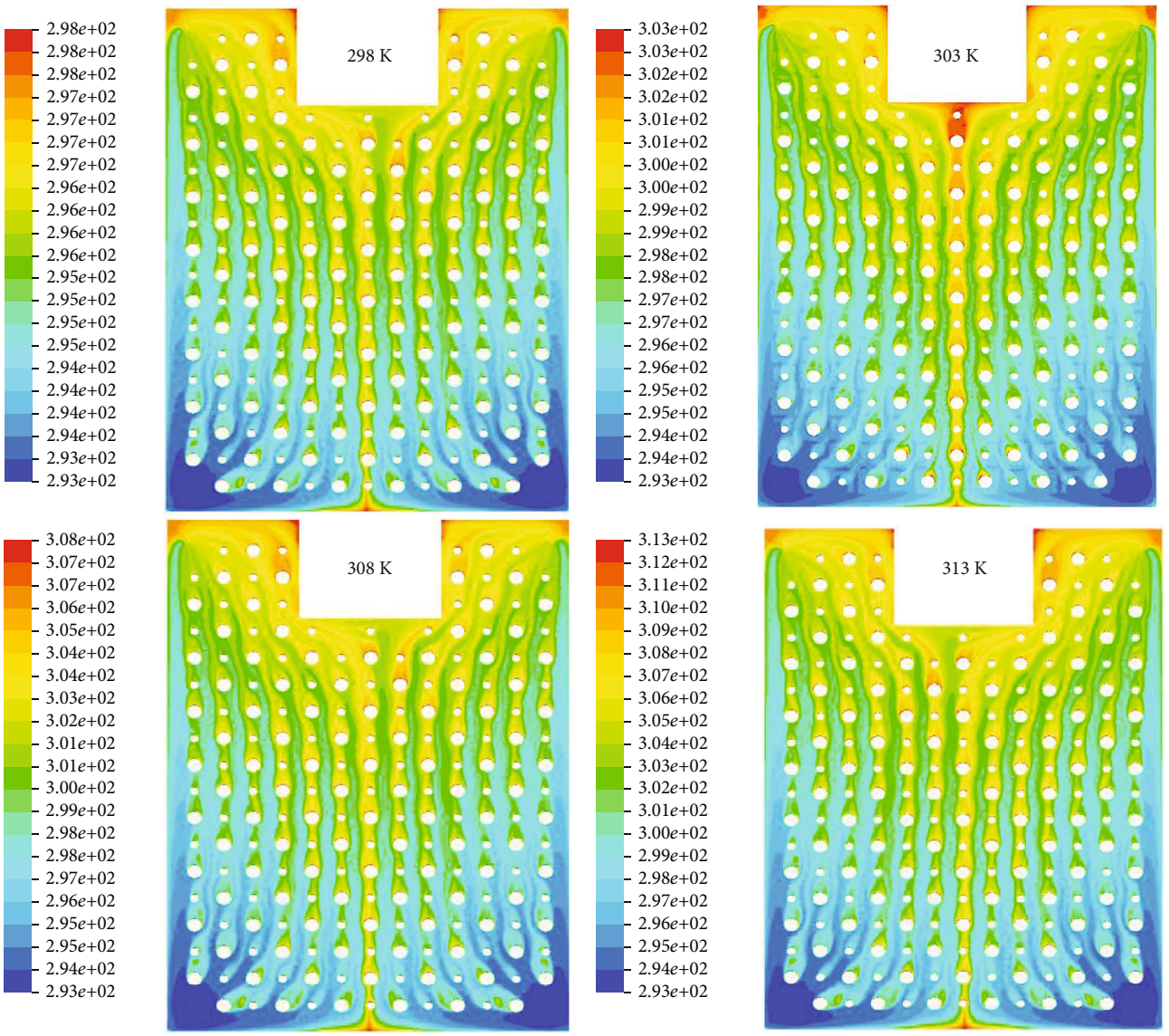

Figure 7: Temperature distribution of water (in K) at different heating surface temperatures.

Abdin and Rachid [33]. It was also found that the PV efficiency drops with the rise in the PV panel temperature.

3.2. Effect of the Geometry Parameters

3.2.1. Corrugation Number. Two ways to change the corrugation number were investigated in this study. One is removing all the small corrugations and keeping all the large corrugations retained (Figure 10), and the other is removing all the large corrugations and keeping all the small corrugations retained. The panel size, other geometric parameters, model, and boundary conditions remain constant. The outlet temperatures of three types of plates under different inlet velocities are shown in Figure 11.

No matter how the corrugation number changes, the heat transfer performance of the hybrid PV/T collector with corrugations is higher than the flat plate collector, and the changing trend of the outlet temperature is similar. As the inlet velocity increases, the outlet temperature decreases while the heat collection increases. When the water inlet velocity changes from 0.2 to 1.0 m/s, the heat collection is between 15.0 and 44.0 MJ per hour.

The changes in the corrugation number on the hybrid PV/T collector performance are not so significant. The impact of the corrugation number on the outlet temperature and heat collection has a certain relationship with the inlet velocity. The outlet temperature of the absorber plate after removing all the small corrugations is slightly higher compared with the original absorber plate when the inlet velocity is less than 0.4 m/s or more than 0.7 m/s. However, when the inlet velocity is between 0.4 m/s and 0.6 m/s (Figure 11), the outlet temperature of the absorber plate after removing all the small corrugations becomes slightly lower than the original absorber plate. While the outlet temperature of the absorber plate after removing all the large corrugations is slightly higher when the inlet velocity is less than 0.45 m/s, it is slightly lower when the inlet velocity is more than 0.45 m/s (Figure 11).

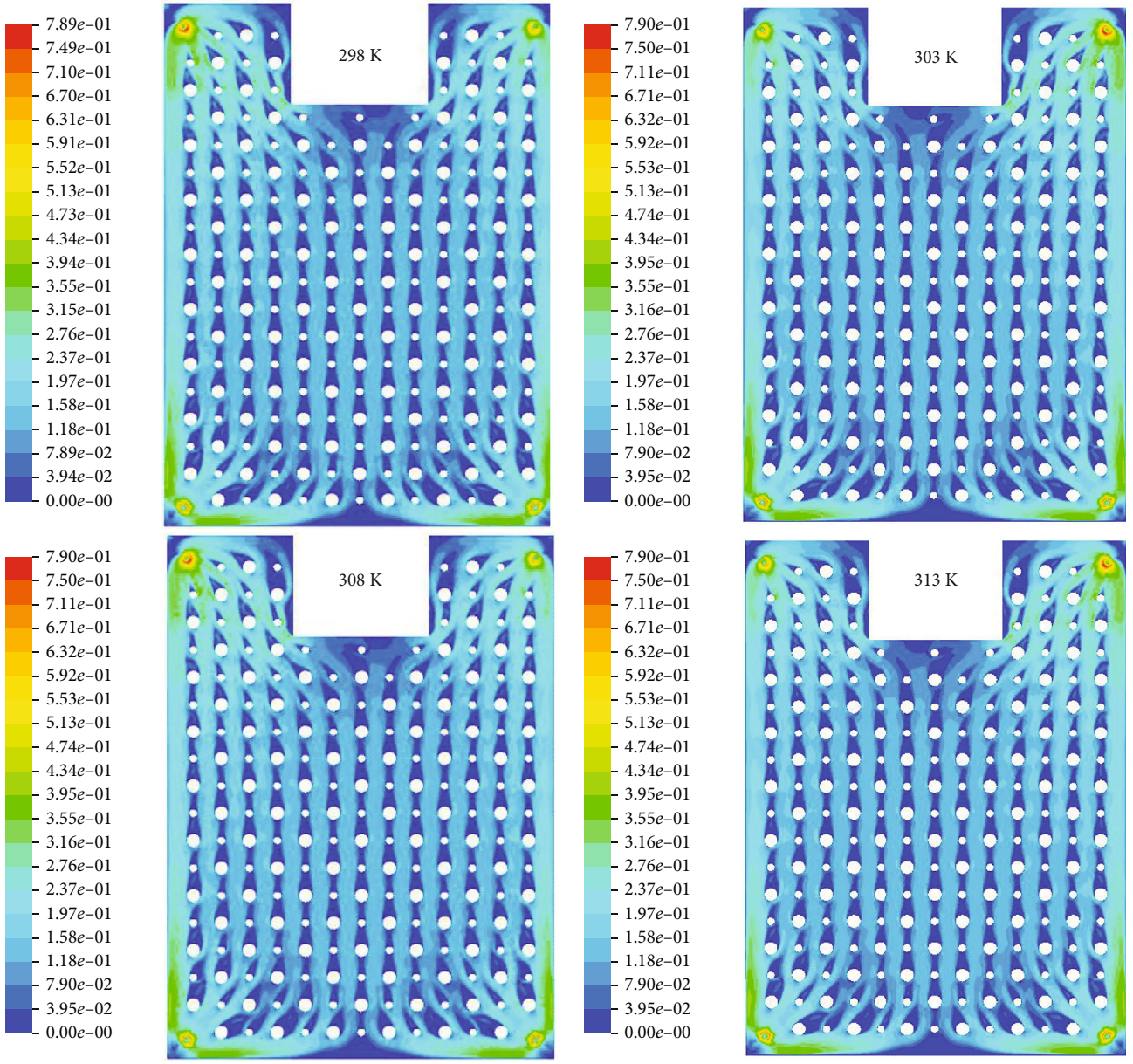

Figure 8: Velocity distribution of internal working fluids (in m/s) at different heating surface temperatures.

The differences in the shape of the collector surface have a direct impact on the flow of the heat transfer fluid and the overall heat transfer coefficient [32]. Removing all the small or large corrugations will increase the contact area between the fluid and the absorber plate and thus lead to sufficient heat transfer. However, it also decreases the flow disturbances between the two panels, leading to a weakened heat transfer. A previous study [34] also reported that the presence of sinusoidal corrugations provides higher flow disturbances, resulting in a significant enhancement in heat transfer. On the other hand, the influence of the corrugation number on the outlet temperature could be offset by the changes in the inlet velocity. That is why the impact of the changes in the corrugation number on the hybrid PV/T collector performance is not so significant.

3.2.2. Corrugation Area. Two ways to change the corrugation area were studied in this work. One is changing all the small corrugations to the large ones (Figure 12), and the other is changing all the large corrugations to the small ones. The panel size, other geometric parameters, model, and boundary conditions are the same as with the original absorber plate. The outlet temperature and heat collection of three types of plates under different inlet velocities are shown in Figure 13.

As shown in Figure 13, as the inlet velocity increases, the outlet temperature gradually decreases, and the decreasing amplitude comes to a lower level. When the inlet velocity changes from 0.2 to 1.0 m/s, the outlet temperature of the absorber plate with all small corrugations changed to the large ones is between 301 and 298 K, and the heat collection

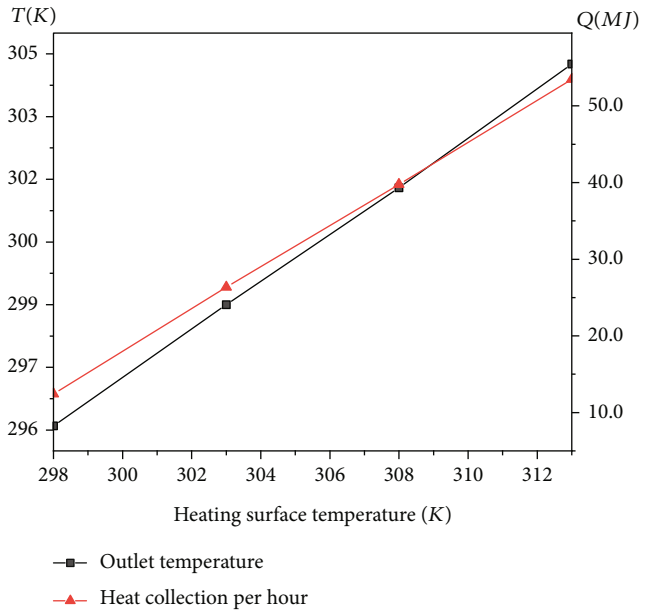

Figure 9: Outlet temperature and heat collection at different heating temperatures.

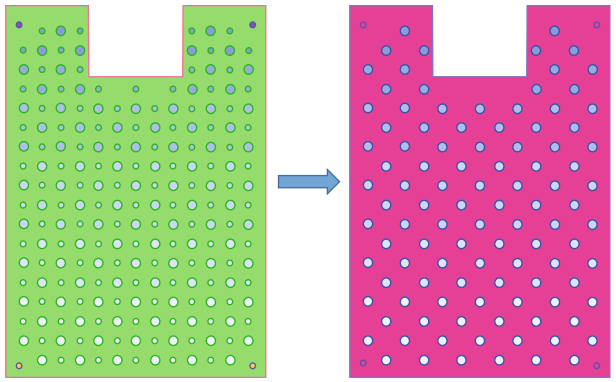

Figure 10: Heat absorber plate with removing all the small corrugations (right).

is in the range of 14.8 to 46.2 MJ/h. Compared with the original heat absorber plate, the heat collection per hour increases gradually at the same flow velocity, and the maximum increment of heat collection is 6.6%. While the absorber plate's outlet temperature is between 301 and 297 K after changing all large corrugations to the small ones, the heat collection is in the range of 14.7-35.7 MJ/h (Figure 13).

With the inlet velocity changing, the outlet temperature of the original plate and the plate with changing corrugation area is significantly higher than the flat plate. When the inlet velocity is greater than 0.4 m/s, the outlet temperature of the heat absorber plate with all small corrugations changing to the large ones is higher than the original plate (Figure 13). However, when the inlet velocity is greater than 0.5 m/s, the outlet temperature of the present absorber plate after changing all large corrugations to the small ones is lower than the original plate (Figure 13).

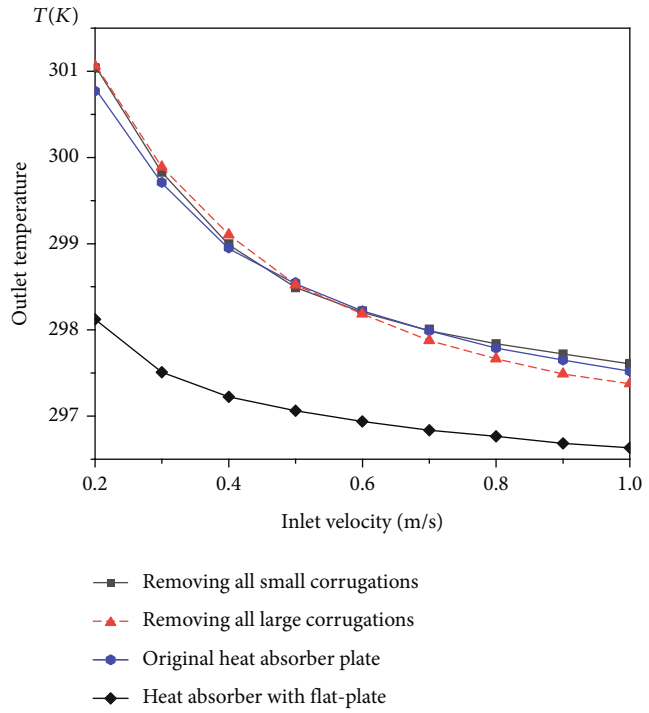

Figure 11: Outlet temperature comparison of three types of absorber plates after changing the corrugation number.

The outlet temperature increased after changing the corrugation area, especially after changing all small corrugations to the large ones when the inlet flow velocity was greater than 0.4 m/s. Besides, due to the flow around the corrugations, the internal water was heated by the back-facing of the PV plate, which was also heated by the increased corrugations. The PV temperature decreases with the increase in the water inlet velocity. Moreover, changing the corrugation area especially changing all large corrugations to the small ones could increase the contact area between the water and the absorber panel. However, it also reduces the flow disturbances caused by the corrugations.

The mass flow rate considered in this study is based on the previously reported experimental evaluation of the PV/T panel, employing a nominal mass flow rate of 0.83 L min^{-1} m^{-2} and a maximum mass flow rate of 3.83 L min^{-1} m^{-2}. Previous studies [22, 30] reported that increasing the fluid flow rate leads to a lower outlet temperature and a higher thermal efficiency of the PV/T panel. It also reported that the experimental thermal efficiency will reach its "optimum point" at a mass flow rate of 5 L/min [22]. Therefore, the PV/T panel exhibits an optimal mass flow rate at a certain solar irradiance. The optimal mass flow rate and the structural parameters, such as the corrugation number and the area, will be considered in the subsequent applied study, referring to the local solar irradiance in combination with the mass flow rate to obtain the high thermal efficiency. Therefore, changing corrugation area does affect the absorber plate performance to a certain extent, but the optimal corrugation area that improves the heat transfer characteristics should be further studied.

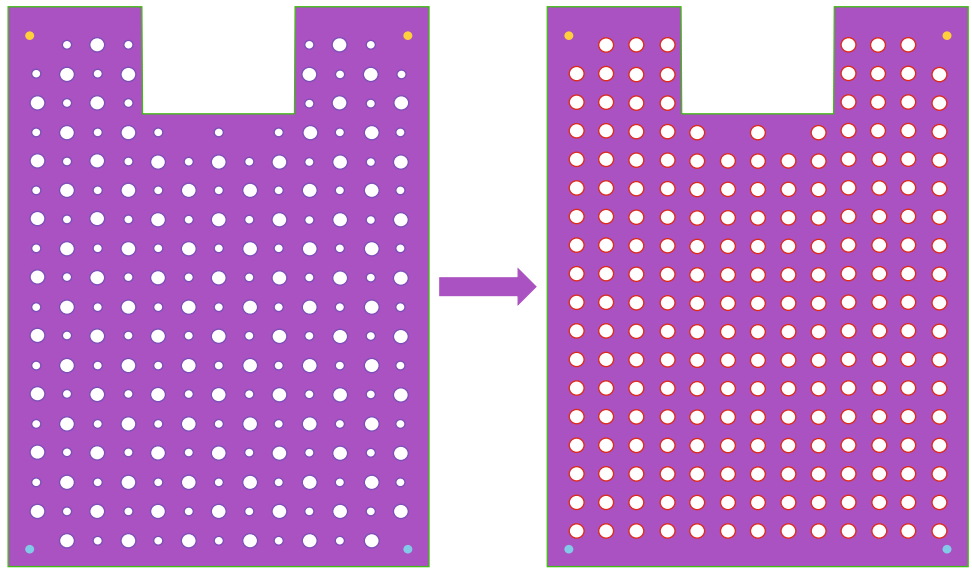

Figure 12: Heat absorber plate with changing all small corrugations to large ones (right).

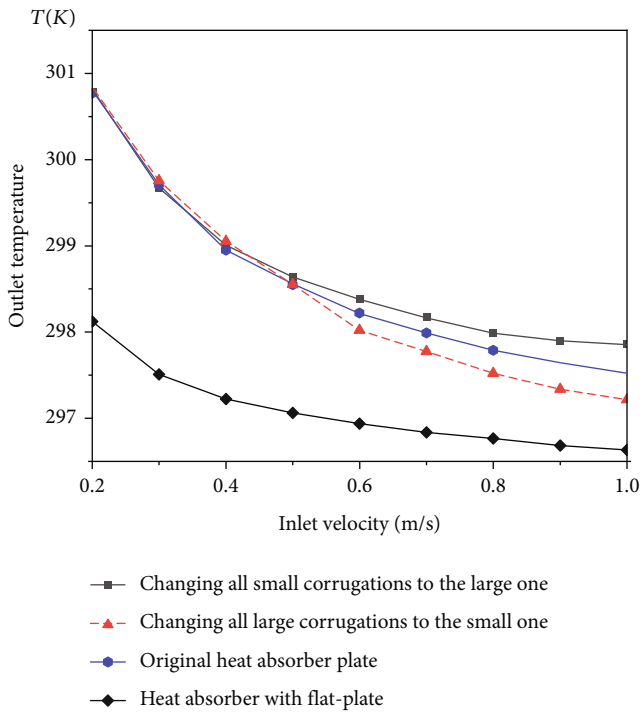

Figure 13: Outlet temperature comparison of three types of absorber plates after changing corrugation area.

3.2.3. Flow Channel Width. Two ways to change the flow channel width were implemented in this study. One is changing the width from 4 to 5 mm (Figure 14(a)), and the other is changing to 3 mm (Figure 14(b)). The plate size, other geometric parameters, model, and boundary conditions are the same as for the original plate. The outlet temperature and heat collection of three types of absorber plates under different inlet velocities are shown in Figure 14.

As shown in Figure 15, as the flow velocity increases, the outlet temperature gradually decreases. When the inlet velocity changes from 0.2 to 1.0 m/s, the outlet temperature of the plate with a 5 mm width is between 297 and 302 K, and the heat collection is in the range of 16.1-39.2 MJ/h. Compared to the original absorber plate, when the inlet velocity is less than 0.3 m/s, the outlet temperature of the plate with a 5 mm width flow channel is higher. On the other hand, the outlet temperature is lower than that of the original absorber plate when the inlet velocity is greater than 0.4 m/s.

The outlet temperature of the absorber plate with a 3 mm width flow channel is significantly higher than both the flat plate and the original plate at different inlet velocities, which is between 298 and 302 K. The heat collection is in the range of 16.3-51.4 MJ/h. Compared with the original PV/T panel, the heat collection per hour increases gradually at the same flow velocity, and the maximum increment in heat collection is 18.6%. This may be owing to the corrugations and narrow flow channel increasing flow obstruction. The presence of corrugations provides higher flow disturbances and pressure drop increases with the decrease in the fin spacing, leading to significant enhancement in heat transfer [34, 35].

The heat transfer characteristics of the hybrid PV/T panel could be improved by changing the flow channel width from 4 mm to 3 mm. Regardless of the employed velocity, the outlet temperature of the absorber plate with a 3 mm flow channel width is higher than that of an absorber plate with a 4 mm channel width. However, the best channel width to enhance the performance of the heat absorber plate should match the corrugation number and area. The collector structure could be optimized when the heat collection generated by changing corrugation area and corrugation number, combined with the heat caused by changing the flow channel width, is positive, which will be carried out in the follow-up study.

Above all, the flow channel width has influences on outlet temperature and heat collection of the hybrid PV/T panel. The heat transfer performance of the hybrid PV/T

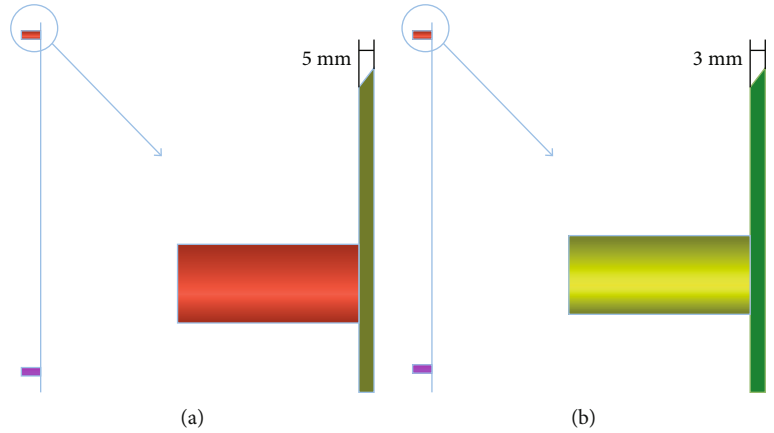

Figure 14: (a) 5 mm width flow channel and (b) 3 mm width flow channel.

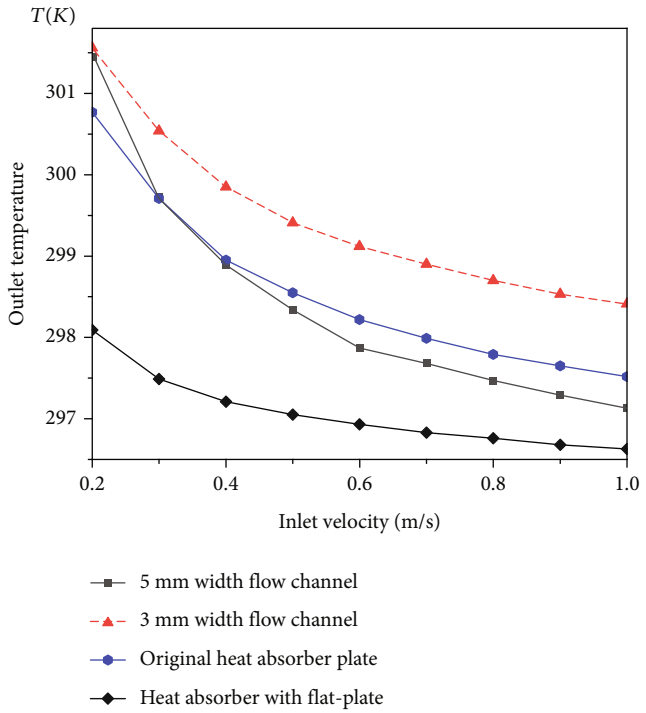

Figure 15: Outlet temperature comparison of three types of absorber plates after changing the flow channel width.

collector with corrugations is higher than the flat plate collector no matter how to change its relevant parameters, which accords with the previous study [34] that also reported that the PV/T panel could enhance thermal efficiency compared to the stand-alone PV panel.

4. Conclusion

In this study, the steady-state flow and heat transfer characteristics of a hybrid PV/T collector with corrugated channels were investigated numerically to investigate the influence of the inlet velocity and heating surface temperature on the thermal performance of the PV/T collector. In order to support the structural optimization of the heat absorber plate to improve the heat collection efficiency, the influences of the structural parameters such as corrugation number, corrugation area, and flow channel width on the heat transfer characteristics were also discussed. The numerical results indicated that

(1) compared with the collector with a flat plate, the outlet temperature of the hybrid PV/T panel with the added corrugations is significantly increased

(2) the outlet temperature and heat collection of the hybrid PV/T panel are affected by the water inlet velocity, corrugated area, and flow channel width

(3) when the inlet velocity is greater than 0.4 m/s, the outlet temperature of the collector plate with all the small corrugations changed to the large ones is higher than the original heat absorber plate, enhancing the heat collection

(4) as the width between the two plates of the hybrid PV/T collector decreases from 4 mm to 3 mm, the improvement of flow heat transfer characteristics significantly leads to the performance enhancement of the heat collection

This study is complementary to the previous studies [30, 31], is limited to the comprehensive effect of the structure parameters of the built-in corrugated channels on the flow and heat transfer, and expands the library of comprehensive evaluation and optimal design of the built-in corrugated channels. The use of a particular absorber is considered based on its uniformity, pressure drop, heat transfer area, mass flow rates, etc. In future investigations, the optimal corrugation number, corrugation area, and flow channel width will be combined with laboratory measurements for a more comprehensive and detailed evaluation.

Data Availability

Some or all data, models, or codes that support the findings of this study are available from the corresponding author upon reasonable request.

Conflicts of Interest

The authors declare that they have no conflicts of interest.

Acknowledgments

This work was funded by the Fundamental Research Funds for the Central Universities (Nos. 3142019017 and 3142021005) and supported by the Higher Education Teaching Reform Research and Practice Project of Hebei Province (No. 2018GJJG479).

References

[1] M. Chandrasekar and T. Senthilkumar, "Five decades of evolution of solar photovoltaic thermal (PVT) technology - a critical insight on review articles," *Journal of Cleaner Production*, vol. 322, article 128997, 2021.

[2] A. Herez, H. El Hage, T. Lemenand, M. Ramadan, and M. Khaled, "Review on photovoltaic/thermal hybrid solar collectors: classifications, applications and new systems," *Solar Energy*, vol. 207, pp. 1321–1347, 2020.

[3] N. Goel, R. A. Taylor, and T. Otanicar, "A review of nanofluid-based direct absorption solar collectors: design considerations and experiments with hybrid PV/thermal and direct steam generation collectors," *Renewable Energy*, vol. 145, pp. 903–913, 2020.

[4] S. Kiwan and I. Salim, "A hybrid solar chimney/photovoltaic thermal system for direct electric power production and water distillation," *Sustainable Energy Technologies and Assessments*, vol. 38, article 100680, 2020.

[5] C. Zhang, J. Li, and Y. Chen, "Improving the energy discharging performance of a latent heat storage (LHS) unit using fractal-tree-shaped fins," *Applied Energy*, vol. 259, article 114102, 2020.

[6] A. Fudholi, K. Sopian, M. Gabbasa et al., "Techno-economic of solar drying systems with water based solar collectors in Malaysia: a review," *Renewable and Sustainable Energy Reviews*, vol. 51, pp. 809–820, 2015.

[7] L. Sahota and G. N. Tiwari, "Review on series connected photovoltaic thermal (PVT) systems: analytical and experimental studies," *Solar Energy*, vol. 150, pp. 96–127, 2017.

[8] M. Kosan and M. Aktas, "Performance investigation of a double pass PVT assisted heat pump system with latent heat storage unit," *Applied Thermal Engineering*, vol. 199, article 117524, 2021.

[9] P. Mi, J. Zhang, Y. Han, and X. Guo, "Study on energy efficiency and economic performance of district heating system of energy saving reconstruction with photovoltaic thermal heat pump," *Energy Conversion and Management*, vol. 247, article 114677, 2021.

[10] S. Tiwari, J. Bhatti, G. N. Tiwari, and I. M. al-Helal, "Thermal modelling of photovoltaic thermal (PVT) integrated greenhouse system for biogas heating," *Solar Energy*, vol. 136, pp. 639–649, 2016.

[11] A. Giwa, A. Yusuf, A. Dindi, and H. A. Balogun, "Polygeneration in desalination by photovoltaic thermal systems: a comprehensive review," *Renewable and Sustainable Energy Reviews*, vol. 130, article 109946, 2020.

[12] A. A. Monjezia, Y. Chen, R. Vepa et al., "Development of an off-grid solar energy powered reverse osmosis desalination system for continuous production of freshwater with integrated photovoltaic thermal (PVT) cooling," *Desalination*, vol. 495, article 114679, 2020.

[13] S. T. Pourafshar, K. Jafarinaemi, and H. Mortezapour, "Development of a photovoltaic-thermal solar humidifier for the humidification- dehumidification desalination system coupled with heat pump," *Solar Energy*, vol. 205, pp. 51–61, 2020.

[14] M. Carmona, A. P. Bastos, and J. D. García, "Experimental evaluation of a hybrid photovoltaic and thermal solar energy collector with integrated phase change material (PVT-PCM) in comparison with a traditional photovoltaic (PV) module," *Renewable Energy*, vol. 172, pp. 680–696, 2021.

[15] M. Khodadadi and M. Sheikholeslami, "Numerical simulation on the efficiency of PVT system integrated with PCM under the influence of using fins," *Solar Energy Materials and Solar Cells*, vol. 233, article 111402, 2021.

[16] A. S. Abdelrazik, F. A. Al-Sulaiman, R. Saidur, and R. Ben-Mansour, "A review on recent development for the design and packaging of hybrid photovoltaic/thermal (PV/T) solar systems," *Renewable and Sustainable Energy Reviews*, vol. 95, pp. 110–129, 2018.

[17] G. Wang, B. Wang, X. Yuan, J. Lin, and Z. Chen, "Novel design and analysis of a solar PVT system using LFR concentrator and nano-fluids optical filter," *Case Studies in Thermal Engineering*, vol. 27, article 101328, 2021.

[18] I. Nkurikiyimfura, Y. Wang, B. Safari, and E. Nshingabigwi, "Electrical and thermal performances of photovoltaic/thermal systems with magnetic nanofluids: a review," *Particuology*, vol. 54, pp. 181–200, 2021.

[19] S. Kumar, R. Thakur, A. Singhy, R. K. Tripathi, and M. Sethi, "A review of heat removal mechanism in concentrated PVT systems using beam splitter," *Materials Today: Proceedings*, vol. 50, pp. 952–961, 2022.

[20] R. Tripathi and G. N. Tiwari, "Annual performance evaluation (energy and exergy) of fully covered concentrated photovoltaic thermal (PVT) water collector: an experimental validation," *Solar Energy*, vol. 146, pp. 180–190, 2017.

[21] A. N. Ozakin and F. Kaya, "Effect on the exergy of the PVT system of fins added to an air-cooled channel: a study on temperature and air velocity with ANSYS Fluent," *Solar Energy*, vol. 184, pp. 561–569, 2019.

[22] A. L. Abdullah, S. Misha, N. Tamaldin, M. A. M. Rosli, and F. A. Sachit, "Theoretical study and indoor experimental validation of performance of the new photovoltaic thermal solar collector (PVT) based water system," *Case Studies in Thermal Engineering*, vol. 18, article 100595, 2020.

[23] M. Hissouf, M. Feddaoui, M. Najim, and A. Charef, "Performance of a photovoltaic-thermal solar collector using two types of working fluids at different fluid channels geometry," *Renewable Energy*, vol. 162, pp. 1723–1734, 2020.

[24] M. Yu, F. Chen, S. Zheng et al., "Experimental investigation of a novel solar micro-channel loop-heat-pipe photovoltaic/thermal (MC-LHP-PV/T) system for heat and power generation," *Applied Energy*, vol. 256, article 113929, 2019.

[25] E. Çiftçi, A. Khanlari, A. Sözen, İ. Aytaç, and A. D. Tuncer, "Energy and exergy analysis of a photovoltaic thermal (PVT) system used in solar dryer: a numerical and experimental investigation," *Renewable Energy*, vol. 180, pp. 410–423, 2021.

[26] E. Arslan, M. Aktas, and O. F. Can, "Experimental and numerical investigation of a novel photovoltaic thermal (PV/T)

collector with the energy and exergy analysis," *Jouranl of Cleaner Production*, vol. 276, article 123255, 2020.

[27] J. Yao, W. Liu, Y. Zhao, Y. Dai, J. Zhu, and V. Novakovic, "Two-phase flow investigation in channel design of the roll-bond cooling component for solar assisted PVT heat pump application," *Energy Conversion and Management*, vol. 235, article 113988, 2021.

[28] W. Fan, G. Kokogiannakis, and Z. J. Ma, "A multi-objective design optimisation strategy for hybrid photovoltaic thermal collector (PVT)-solar air heater (SAH) systems with fins," *Solar Energy*, vol. 163, pp. 315–328, 2018.

[29] C. Yu, H. Li, J. Chen, S. Qiu, F. Yao, and X. Liu, "Investigation of the thermal performance enhancement of a photovoltaic thermal (PV/T) collector with periodically grooved channels," *Journal of Energy Storage*, vol. 40, article 102792, 2021.

[30] P. Xu, X. X. Zhang, J. C. Shen, X. Zhao, W. He, and D. Li, "Parallel experimental study of a novel super-thin thermal absorber based photovoltaic/thermal (PV/T) system against conventional photovoltaic (PV) system," *Energy Report*, vol. 1, pp. 30–35, 2015.

[31] Q. P. Li, J. S. Wu, G. J. Wang et al., "Numerical simulation and experimental test of a novel compact solar collector with internally extruded pin-fin flow channel (in Chinese)," *HV & AC*, vol. 50, pp. 103–110, 2020.

[32] A. K. Hussein, T. C. Miqdam, A. H. Al-Waeli, and K. Sopian, "Comparison and evaluation of solar photovoltaic thermal system with hybrid collector: an experimental study," *Thermal Science and Engineering Progress*, vol. 22, article 100845, 2021.

[33] Z. U. Abdin and A. Rachid, "Bond graph modeling of a water-based photovoltaic thermal (PV/T) collector," *Solar Energy*, vol. 220, pp. 571–577, 2021.

[34] M. S. Manjunath, K. V. Karanth, and N. Y. Sharma, "Numerical investigation on heat transfer enhancement of solar air heater using sinusoidal corrugations on absorber plate," *International Journal of Mechanical Sciences*, vol. 138-139, pp. 219–228, 2018.

[35] A. Priyam and P. Chand, "Thermal and thermohydraulic performance of wavy finned absorber solar air heater," *Solar Energy*, vol. 130, pp. 250–259, 2016.